Virtual 2D-3D Fracture Reduction with Bone Length Recovery Using Statistical Shape Models

Ondřej Klíma[1[0000−0001−9295−065X]], Roman Madeja[2[0000−0002−9253−3116]], Michal Španel[1,3[0000−0003−0193−684X]], Martin Čuta[4[0000−0001−6239−383X]], Pavel Zemčík[1[0000−0001−7969−5877]], Pavel Stoklásek[5], and Aleš Mizera[5[0000−0001−9681−1008]]

[1] IT4Innovations Centre of Excellence, Brno University of Technology, Božetěchova 1/2, 612 66 Brno, Czech Republic
{iklima,spanel,zemcik}@fit.vutbr.cz
[2] University Hospital in Ostrava, 17. listopadu 1790, 708 52 Ostrava, Czech Republic
[3] 3Dim Laboratory s.r.o, Kamenice 34, 625 00 Brno, Czech Republic
http://www.3dim-laboratory.cz/
[4] Laboratory of Morphology and Forensic Anthropology, Department of Anthropology, Masaryk University, Kotlářská 2, Brno 611 37, Czech Republic
[5] CEBIA-Tech, Faculty of Applied Informatics, Tomas Bata University in Zlín, Nad Stráněmi 4511, 760 05 Zlín, Czech Republic

Abstract. Computer-assisted 3D preoperative planning based on 2D stereo radiographs has been brought into focus recently in the field of orthopedic surgery. To enable planning, it is crucial to reconstruct a patient-specific 3D bone model from X-ray images. However, most of the existing studies deal only with uninjured bones, which limits their possible applications for planning. In this paper, we propose a method for the reconstruction of long bones with diaphyseal fractures from 2D radiographs of the individual fracture segments to 3D polygonal models of the intact bones. In comparison with previous studies, the main contribution is the ability to recover an accurate length of the target bone. The reconstruction is based on non-rigid 2D-3D registration of a single statistical shape model onto the radiographs of individual fragments, performed simultaneously with the virtual fracture reduction. The method was tested on a syntethic data set containing 96 virtual fractures and on real radiographs of dry cadaveric bones suffering peri-mortem injuries. The accuracy was evaluated using the Hausdorff distance between the reconstructed and ground-truth bone models. On the synthetic data set, the average surface error reached 1.48 ± 1.16 mm. The method was built into preoperative planning software designated for the selection of the best-fitting fixation material.

Keywords: Preoperative planning · Fracture reduction · Fixation devices · 2D-3D registration · Statistical shape model

1 Introduction

Plain radiography plays a key role in bone fracture diagnosis and treatment. In the case of surgical intervention, plain radiographs enable basic preoperative planning, such as bone fracture classification and the determination of an appropriate fixation technique for its stabilization. More advanced, computer-assisted planning of the osteosynthesis provides a virtual simulation of the intervention, which typically includes situating the fracture segments into anatomically correct and mechanically stable poses, measuring the bone morphology, or placing fixation devices [9]. The virtual simulations rely on 3D polygonal models of individual bone fragments, which are conventionally obtained from volumetric images provided by computed tomography (CT). However, during the CT examinations, the patients are exposed to substantially higher doses of radiation in comparison with plain radiography. Therefore, the indication of CT examinations is generally restricted only to cases of severe or complex fractures, while the treatment of rather common cases depends on plain radiographs. Nevertheless, computer-assisted planning can be still beneficial even for rather routine fractures, especially for long bone fractures of the lower limbs. One important contribution is the possibility of preoperative measurement of patient-specific bone morphology with aim of determining the features of the best-fitting fixation devices, such as the length of the intramedullary nail [8], the size of the bone plate, or the number and placement of bone screws. Therefore, a reconstruction of a 3D patient-specific anatomy based only on plain, clinically available radiographs instead of volumetric images is of great importance for the application of virtual planning in a broader spectrum of bone fracture treatment procedures.

In this paper, we propose a semi-automatic 3D virtual fracture reduction method, which is able to reconstruct a polygonal model of an intact bone from stereo radiographic images of the individual fracture segments. The method is focused on displaced diaphyseal fractures of the simple or wedge type.

2 Related Work

In the field of orthopedic surgery, a somewhat similar challenge of computer-assisted 3D preoperative planning based only on plain radiographs was recently addressed by several projects [2,1] focusing on total hip arthroplasty (THA), total knee arthroplasty (TKA), and lower extremity osteotomy. Other studies were focused on observing 3D joint kinematics from fluoroscopy sequences without the requirement of CT image acquisition [5,17,18]. Instead of CT scans, a non-rigid registration of 3D bone atlases onto the stereo radiographs was exploited to reconstruct polygonal models of the bones. As proposed in works such as [15], statistical shape models were involved as the atlases to perform a shape-constrained 2D-3D registration. With respect to the statistical shape models, this reconstruction approach is straightforward when the target bone is not suffering any injuries, which is fulfilled for the total joint arthroplasty or observation of joint kinematics. However, arbitrarily shaped fracture segments make reconstruction based on statistical shape models a challenging task.

The first attempt to reconstruct injured bones using statistical atlases was proposed in a study focused on the reduction of multi-fragment fractures of the distal radius [7]. The goal of the study was to obtain a polygonal model of an intact bone from plain radiographs of the fracture segments. The reconstruction, together with the fracture reduction, were achieved at the same time by a 2D-3D registration of a single statistical appearance model of an intact distal radius into individual fracture segments. Splitting the statistical appearance model into fracture segments was performed automatically by the registration. The method was evaluated *in silico* using simulated fractures, concluding that the atlas-based reconstruction may provide a more accurate distal radius template than the conventionally used mirrored model obtained from the contralateral limb.

A later study, using a similar principle of a multi-fragment 2D-3D registration of a statistical shape model, focused on diaphyseal fractures of the long bones of the lower limbs [16]. In contrast with the previous work, its aim was to determine the rotation alignment between the proximal and distal fragments along the longitudinal axis. In addition to the rotation angles, the study considered the reconstruction of surface models of the individual fracture segments. However, the approach was unable to perform virtual fracture reduction and to provide a model of the intact bone, as the method was unable to determine the correct length of the target bone. Moreover, the shape model had to be divided into fragments in advance, without further refinement during the registration process. The bone length also had to be provided manually in a study focused on automatic fracture reduction using statistical atlases, working with mesh models of fracture segments obtained from CT scans [3].

In this paper, we address the challenge of accurate bone length recovery. Unlike [16], the division of the statistical shape model into segments is performed automatically by the registration, enabling optimization of the shape model length. In consequence, the proposed method is able to perform virtual fracture reduction and provide a 3D model of the intact bone.

3 Method

The method is based on a multi-fragment registration of a statistical shape model into stereo radiographs of individual fracture segments, extended by simultaneous optimization of the shape model length.

3.1 Statistical Shape Models

The statistical shape models involved in this study work as elastic tetrahedral models of bones. As their elasticity is shape-constrained, it is ensured the models always represent anatomically reasonable bones. The shape models involved were created using a procedure detailed in [12]. As the models are based on probabilistic principal component analysis (PPCA), they are represented by the following generative model:

$$S = \phi\mathbf{b} + \overline{S} + \omega \tag{1}$$

Table 1. Characteristics of involved statistical shape models.

Statistical shape model	Size of training set	Modes of variation	Tetrahedral vertices	Tetrahedra
Femur	43 bones	41	20,843	93,480
Tibia	42 bones	40	22,003	106,436

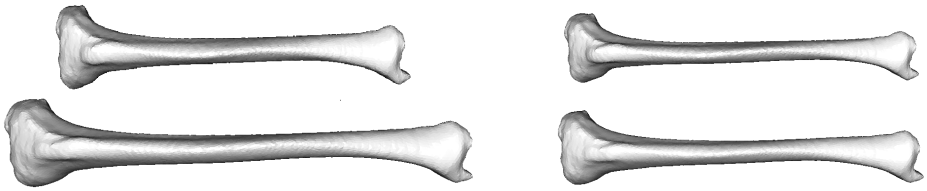

$b_1 = \pm 2\sigma$ $b_2 = \pm 2\sigma$

Fig. 1. Statistical shape model of the tibia. The instances were generated by setting the first *(left)* and the second *(right)* parameter to $\pm 2\sigma$. The rest of the modes were set to zero.

where S is a vector containing tetrahedral vertices of the model, the shape of which is determined by independent modes of variation $\mathbf{b}$; $\overline{S}$ is a tetrahedral model of the mean bone; ϕ is a matrix of the principal components; and ω describes zero-meaned Gaussian noise.

Two statistical shape models, representing the femur and tibia, were created using CT images of intact bones, provided by the University Hospital in Ostrava. The characteristics of the models are shown in Table 1. Both tetrahedral models include a polygonal surface, formed by $19,996$ faces and by a subset counting $10,000$ tetrahedral vertices.

As previously described in [3], the length of the femoral or tibial shaft is relatively independent of the shape of the joint regions. Considering the statistical shape models of the involved bones, the length of the shaft is controlled mainly by the first mode b_1, while features such as the size or shape of the joint regions are modeled in particular by the rest of the modes $b_2 \dots b_n$ (Fig. 1). Therefore, it is impossible to determine the length of a bone based only on the shape of its distal and proximal parts.

3.2 Reconstruction

The reconstruction outcome comprises a model of a patient-specific intact bone, described by shape modes $\mathbf{b}$, and poses $p_{\text{prox}}, p_{\text{dist}}$ of both fracture segments, forming a vector $\mathcal{P} = (\mathbf{b}, p_{\text{prox}}, p_{\text{dist}})$. The results are obtained by minimization of the reprojection error, evaluated using a nonoverlapping area measure (NOA), together with a length criterion (LC):

$$(\mathcal{P}^*) = \arg\min_{\mathcal{P}} \Big[\text{NOA}(\mathcal{P}) + \text{LC}(\mathcal{P})\Big] \tag{2}$$

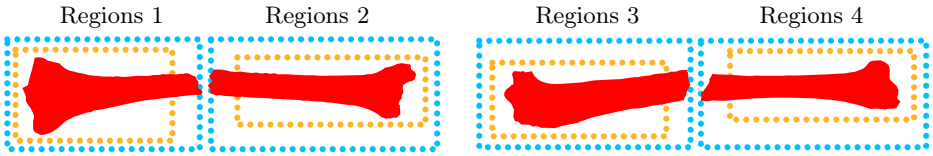

Fig. 2. The input radiographs are divided into different regions of interest. The regions related to nonoverlapping area evaluation *(orange)* border the maximal intact parts of the bones. The boundaries of regions for length estimation *(blue)* are determined with respect to the detachement point of the bone fragments. The regions are estimated as scaled-up bounding boxes of the fragment segmentations, except the sides nearest to the fracture, which are set interactively by the user.

Both terms are evaluated using the input radiographs, though with different regions of interest (Fig. 2).

Nonoverlapping Area. The measure is evaluated between binary segmentations of the input digital radiographs (DR) and digitally reconstructed radiographs (DRR)[12] with a reprojected statistical shape model, using only the intact regions of the bones. The nonoverlapping area is defined as the area that the segmentations do not have in common (Fig. 3). As shown in [13], it can be evaluated as a sum of the squared pixel differences (PD) between the input and virtual segmentations:

$$\mathrm{d}(\mathcal{P}, x, y) = \mathrm{DR}(x, y) - \mathrm{DRR}(\mathcal{P}, x, y) \tag{3}$$

$$\mathrm{PD}(\mathcal{P}) = \big(\mathrm{d}(x_1 \dots x_n, y_1 \dots y_m)\big) \tag{4}$$

$$\mathrm{NOA}(\mathcal{P}) = \|\mathrm{PD}(\mathcal{P})\|^2 \tag{5}$$

Instead of a count of different pixels, it is convenient to express the size of the nonoverlapping area relatively as $\frac{\mathrm{NOA}(\mathcal{P})}{\mathrm{NOA}(\mathcal{P})+\mathrm{OA}(\mathcal{P})}$, where $\mathrm{OA}(\mathcal{P})$ is the size of the overlapping area. The measure is an intensity-based similarity metric in the sense that the evaluation is perfomed directly with the input and reprojected pixels, leading to correspondence-free registration [13]. In contrast, the feature-based methods [6,5] usually require establishing correspondences between the shape model vertices and the contours detected in the radiographs, which is a challenging and error-prone task.

Bone Length Recovery. As the method works with simple or wedge fractures, the injured bone is split into two main fragments. Each fragment is captured in two regions of interest forming a stereo pair, as shown in Fig. 2. The key idea of the recovery is to assign each vertex of the shape model to only one of the main fragments. In consequence, each vertex should be reprojected in precisely two regions, which is achieved by minimizing the length criterion:

$$\mathrm{RV}(\mathcal{P}) = \big(\mathrm{r}(\mathcal{P}, v_1 \dots v_n) - 2\big) \tag{6}$$

$$\mathrm{LC}(\mathcal{P}) = \|\mathrm{RV}(\mathcal{P})\|^2 \tag{7}$$

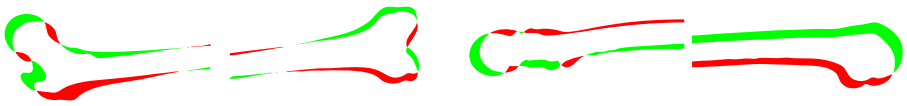

Anterior-posterior view Lateral view

Fig. 3. Nonoverlapping area between the input *(red)* and virtual *(green)* segmentations. The size of the depicted nonoverlapping area is 28.5%.

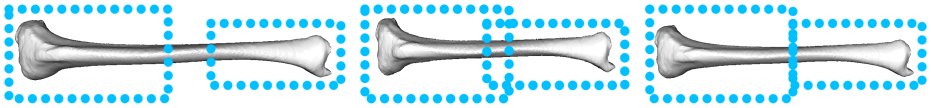

Too long Too short Correct length

Fig. 4. Relation between vertex assignment and resulting bone length. No assignment of the vertices in the middle of the shaft to any of the fragments leads to a bone that is too long *(left)*. Assignment of the vertices to both fragments results in a bone that is too short *(middle)*. The correct length is ensured by assigning each vertex to exactly one fragment *(right)*.

where $\mathrm{r}(\mathcal{P}, v)$ is the number of reprojections of the current vertex v. The relation between misassigned vertices and bone length is shown in Fig. 4. The regions of interest for the length recovery must be set with respect to a point of detachement (Fig. 2).

Optimization Scheme. The registration is solved as a non-linear least squares (NLS) problem, using a numerical Levenberg-Marquardt optimizer [10]. Although a computationally demanding approximation of the Jacobian matrix is required, due to its high rate of convergence, the optimizer is able to outperform stochastic gradient-free methods [14]. The Jacobian matrix J_F has the following form:

$$J_F = \begin{pmatrix} \partial \mathrm{PD}_{\mathtt{prox}}(\mathcal{P}) / \partial p_{\mathtt{prox}} & 0 & \partial \mathrm{PD}_{\mathtt{prox}}(\mathcal{P}) / \partial \mathbf{b} \\ 0 & \partial \mathrm{PD}_{\mathtt{dist}}(\mathcal{P}) / \partial p_{\mathtt{dist}} & \partial \mathrm{PD}_{\mathtt{dist}}(\mathcal{P}) / \partial \mathbf{b} \\ \partial \mathrm{RV}(\mathcal{P}) / \partial p_{\mathtt{prox}} & \partial \mathrm{RV}(\mathcal{P}) / \partial p_{\mathtt{dist}} & \partial \mathrm{RV}(\mathcal{P}) / \partial \mathbf{b} \end{pmatrix} \tag{8}$$

where the partial derivates are approximated using central differences as $\partial f(t) / \partial t \approx f(t+\epsilon) - f(t-\epsilon) / 2\epsilon$.

The reconstruction is divided into three subsequent optimizations. At first, only poses $p_{\mathtt{prox}}, p_{\mathtt{dist}}$ are considered. Next, the first five shape modes $b_1 \dots b_5$ are optimized together with the poses. Finally, all modes $\mathbf{b}$ are involved in the last stage. Before the optimization, a rough initial pose of the statistical shape model together with the regions of interest must be set interactively by the user, or estimated from the segmentations, as described in the following sections. The binary segmentations of the input radiographs are performed manually. The modes of variation of the shape model are initialized to zeros.

4 Results

The accuracy and performance of the proposed method were evaluated on synthetic X-ray images of simulated fractures and on real radiographs of dry cadaveric bones suffering perimortem injuries. To evaluate the accuracy, the differences between the polygonal models reconstructed by the proposed method, and ground-truth surfaces obtained from CT data sets were measured using the symmetric Hausdorff distance [4]. The CT data sets of ground-truth bones were never included into the training sets of the statistical shape models. Following the reconstruction convergence criterion stated in [6], the method converged in each evaluated case, as the RMS error was always lower than 3 mm. The ϵ for the Jacobian matrix approximation was set to 1 mm or 1° in the case of pose parameters and to 1 standard deviation σ for shape modes $\mathbf{b}$, as previously proposed in [12].

The evaluations were performed using a 64-bit Windows 7 desktop machine, equipped with an Intel i5 processing unit, NVidia GTX 980Ti 6 GB graphics adapter and 24 GB DDR4 RAM.

4.1 Simulated Injuries

For the *in silico* evaluation of the fracture reduction, we adopted a data set of virtual X-ray images, previously presented in [12]. The virtual radiographs were ray-casted from 8 already segmented CT images of femoral bones obtained from the `Virtual Skeleton Database (VSD)` [11]. From each CT image, 12 virtual stereo pairs of orthogonal radiographs were created, resulting in 96 cases in total. As the bones were rotated 30° along the longitudinal axis between the individual renderings, the data set contained X-ray images captured even from arbitrary views, in addition to standard anterior-posterior and lateral radiographs. The source-image distance (SID) was set to exactly 1 meter; the pixel spacing of the radiographs was set to 0.75 mm. To simulate transversal fractures of the femoral shaft, each radiograph was split into proximal and distal parts. A sample test case chosen from the evaluation data set is shown in Fig. 5.

Initial poses of the statistical shape model were generated randomly, with uniform distribution and maximum difference to the ground-truth poses limited to ± 10 mm and $\pm 10°$, respectively.

Fig. 5 shows the result of the virtual fracture reduction of the sample test case. As the virtual radiographs and the reference polygonal models were obtained from the same CT images, the reconstructed bones were compared directly with ground-truth surfaces. The accuracy evaluation for each bone, together with the size of the nonoverlapping area, the number of misassigned tetrahedral vertices, and the length error, as well as the performance evaluation, including the overall reconstruction time, number of iterations in each stage and a total number of rendered images, are shown in Table 2. The results for each bone were averaged from 12 evaluations using different stereo radiographic pairs.

The virtual reduction method extends the *Black & White Pixel Differences* (BW-PD) approach proposed in [12], designated for a single-fragment 2D-3D

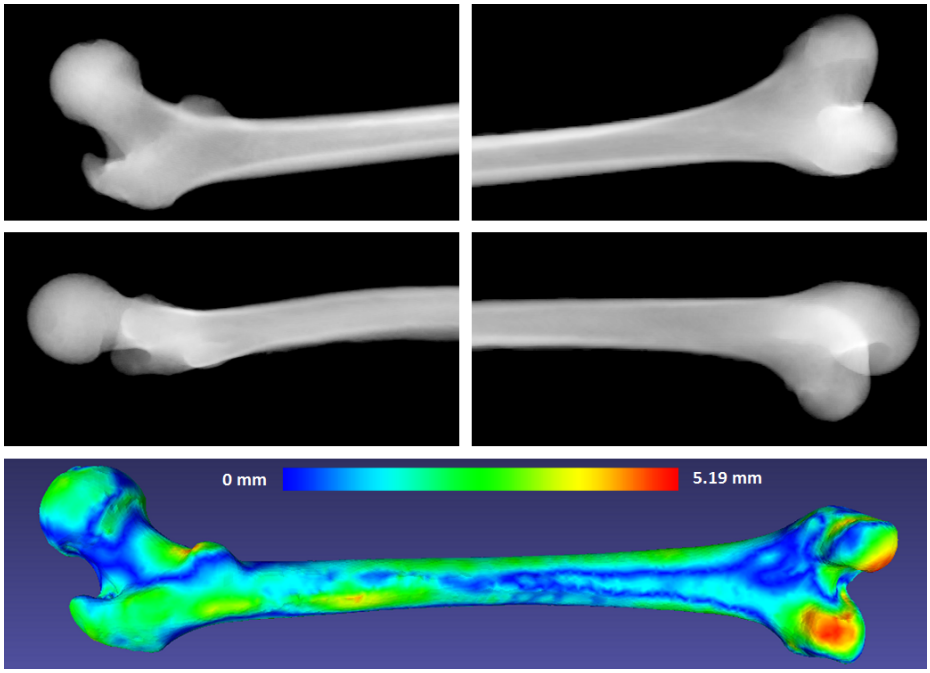

Fig. 5. A sample test case of stereo radiographs with simulative transversal fracture of the femoral shaft, chosen from the virtual data set *(top)*. Accuracy of the sample case reconstruction *(bottom)*. The heatmap shows the differences between reconstructed and ground-truth surfaces, evaluated using the symmetric Hausdorff distance.

reconstruction of the uninjured bones. Evaluated on the same synthetic data set, the `BW-PD` method reached an average accuracy of 1.02 ± 1.35 mm when reconstructing the uninjured bones, while the proposed method reached 1.48 ± 1.16 mm when performing virtual reduction of simulated shaft fractures.

4.2 Dry Cadaveric Bones Study

The cadaveric study involved archeological bones, two femoral and one tibial, suffering peri-mortem diaphyseal fractures. A sample bone from the study is shown in Fig. 6. The radiographs of individual fragments were taken sequentially, using a Kodak Carestream Directview DR 9500 System imaging system. Two CR X-ray cassettes with dimensions of 35×43 cm and 0.168 mm pixel spacing were exploited for the captures. The source-image distance was set to approximately 1 meter. The radiographs were calibrated using a custom made radiostereometric biplanar calibration box, described in detail in [13]. The complete experimental set up for capturing radiographs is shown in Fig. 6. Individual bone fragments, sealed in a foil sleeve, were placed approximately in the center of the box, on Styrofoam underlays. Contrary to the synthetic data set, the radiographs were

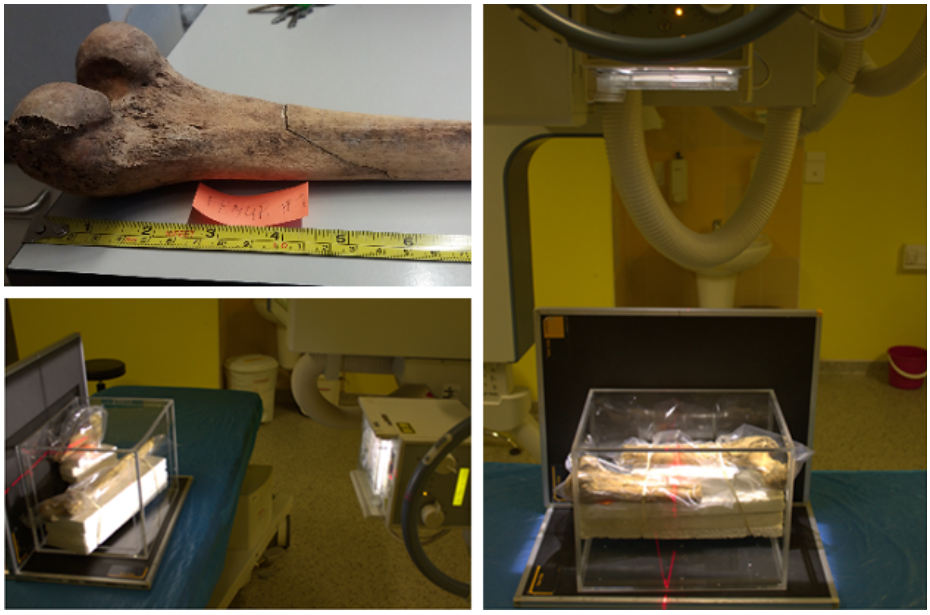

Fig. 6. Physically reduced dry cadaveric femur involved in the study *(top-left)*, capturing an anterior-posterior radiograph of the experimental setup *(right)*, taking a lateral radiograph *(bottom-left)*.

taken only from the anterior-posterior and lateral views. After capturing the radiographs, the fractures were actually reduced and fixed by gluing individual fragments together. Then, the reference polygonal models were obtained from CT images of the reduced bones. The poses of the statistical shape model were initialized interactively in a custom viewer.

In contrast with the *in silico* study, rigid registration of the reconstructed bones onto the reference models had to be performed before the Hausdorff distance evaluation. The results of the evaluation are shown in Table 2, revealing a slight decrease in accuracy for the cadaveric bones. The accuracy was affected by the manual segmentation and the real-world calibration of the radiographic images; the higher RMS error in comparison with the simulative data set was caused by certain degradations of the archeological bones involved. The higher number of misassigned tetrahedral vertices was related to a user estimation of the separation spot, which was, by contrast, ideal in the case of the *in silico* study.

4.3 Preoperative Planning Software

The method has been built into preoperative planning software, which provides a large database of 3D models capturing bone plates and intramedullary nails. The user is able to select the intended device from the database, place it interac-

Table 2. Results of the reconstruction accuracy and performance evaluation.

Bone	Nonoverlapping area (%)	Misassigned vertices	Length error (mm)	Mean Hausdorff distance (mm)	RMS error
VSD identif.	*Simulated fractures*				
226	2.34	11.0	0.57	1.28	0.99
230	2.38	6.3	1.06	1.23	0.95
238	2.60	10.3	0.49	1.61	1.27
254	2.56	13.3	2.16	1.54	1.20
5900	2.85	6.7	4.07	1.31	1.02
5953	2.60	3.7	2.77	1.41	1.09
6009	2.85	8.1	1.44	1.70	1.35
5939	3.33	15.0	0.94	1.78	1.43
	Perimortem fractured dry cadaveric bones				
Femur 1	3.41	86	3.8	1.89	2.16
Femur 2	2.33	50	3.1	1.38	1.70
Tibia	3.50	131	2.0	1.73	2.16

Bone	Overall time (mm:ss)	Iterations			Renderings
		Stage 1	Stage 2	Stage 3	
VSD identifier	*Simulated fractures*				
226	1:54.4	55.6	16.3	12.9	9,609
230	1:59.0	48.8	21.7	14.8	10,454
238	2:15.2	63.3	21.1	15.0	11,248
254	3:55.2	84.0	79.6	22.5	20,550
5900	3:04.5	80.2	66.3	12.7	15,387
5953	2:11.1	56.5	20.1	15.9	11,149
6009	2:57.6	66.1	58.5	16.3	15,343
5939	2:11.9	67.9	40.3	10.6	11,583
	Perimortem fractured dry cadaveric bones				
Femur 1	3:49.3	11	48	38	19,752
Femur 2	2:16.7	42	24	21	12,684
Tibia	1:13.0	17	34	13	9,160

tively onto the reconstructed bone model, possibly to perform a virtual bending of the bone plate, and finally refine its pose using an automatic procedure. The application also provides the cutting planes of the obtained polygonal model as a tentative approximation of the fracture detachment sites, or measurements of required screw lengths (Fig. 7). A mutual pose of stereo radiographs is determined using a calibration marker, which is usually attached to a lower limb splint. The shape model is initially aligned with the longitudinal axes of fragments, which are reconstructed in 3D from the binary segmentations.

5 Discussion and Conclusions

In this paper, we proposed a method for a virtual 2D-3D reduction of shaft fractures of the lower limbs. To the best of our knowledge, no other method considering multifragment 2D-3D reconstruction with a focus on accurate length estimation has been proposed so far. The accuracy of the method is compara-

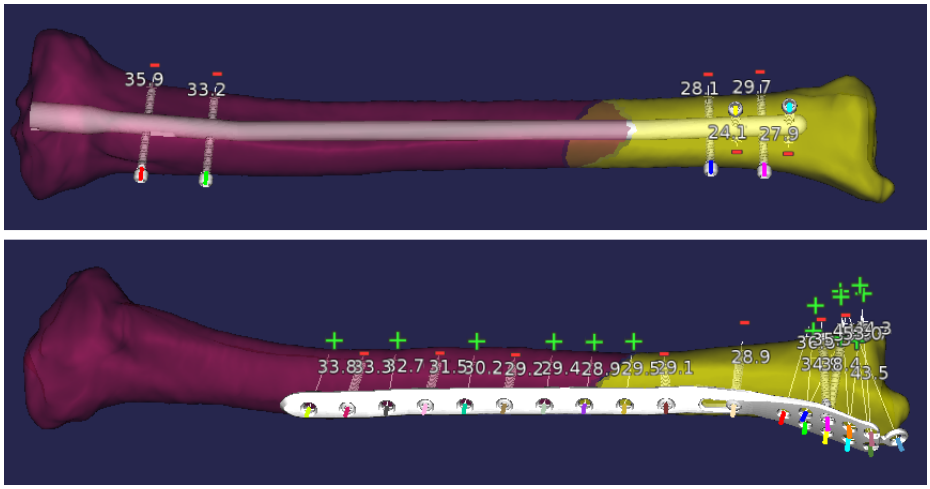

Fig. 7. A virtual simulation of intramedullary nailing of a tibial shaft fracture *(top)*, and a virtual placement of a distal tibial bone plate *(bottom)*. The bone model was reconstructed from radiographs of a real traumatology case.

ble even with single-fragment reconstruction approaches, presented in a brief summary in [6]. The results revealed that the accuracy and performance are sufficient for involvement in preoperative planning software designed for the selection of the best-fitting fixation material. To omit the manual segmentation of input radiographs, which is a time-consuming and subjective task, the future work will focus on replacing the nonoverlapping area measure with density-based registration. We assume that the length estimation based on assigning the statistical shape model vertices to individual bone fragments is straightforwardly generalizable, even for application in virtual fracture reduction using 3D models of the fragments obtained from CT images, as proposed e.g. in [3]. The reconstruction method is distributed as open-source library and front-end application at `https://github.com/klepo/libmultifragmentregister`.

Acknowledgements. This work was supported by the Technology Agency of the Czech Republic Grant No. TE01020415 V3C - Visual Computing Competence Center and by the Ministry of Education, Youth and Sports of the Czech Republic within the National Sustainability Programme project No. LO1303 (MSMT-7778/2014).

References

1. iJoint: 2D/3D reconstruction of patient-specific hip joint from conventional X-ray radiographs. `http://www.istb.unibe.ch/research/information_processing_in_medical_interventions/ijoint/index_eng.html`, Accessed: 2018-08-08
2. iLeg: 2D/3D reconstruction of lower extremity from clinically available X-rays. `http://www.istb.unibe.ch/research/information_processing_in_medical_interventions/ileg/index_eng.html`, Accessed: 2018-08-08

3. Albrecht, T., Vetter, T.: Automatic Fracture Reduction. In: Levine, J.A., Paulsen, R.R., Zhang, Y. (eds.) Mesh Processing in Medical Image Analysis 2012. pp. 22–29. Springer Berlin Heidelberg, Berlin, Heidelberg (2012)
4. Aspert, N., Santa-Cruz, D., Ebrahimi, T.: MESH: measuring errors between surfaces using the Hausdorff distance. In: Multimedia and Expo, 2002. ICME '02. Proceedings. 2002 IEEE International Conference on. vol. 1, pp. 705–708 (2002)
5. Baka, N., de Bruijne, M., van Walsum, T., Kaptein, B.L., Giphart, J.E., Schaap, M., Niessen, W.J., Lelieveldt, B.P.F.: Statistical Shape Model-Based Femur Kinematics From Biplane Fluoroscopy. IEEE Transactions on Medical Imaging **31**(8), 1573–1583 (Aug 2012)
6. Baka, N., Kaptein, B., de Bruijne, M., van Walsum, T., Giphart, J., Niessen, W., Lelieveldt, B.: 2D-3D shape reconstruction of the distal femur from stereo X-ray imaging using statistical shape models. Med. Image Analysis **15**, 840 – 850 (2011)
7. Gong, R.H., Stewart, J., Abolmaesumi, P.: Reduction of multi-fragment fractures of the distal radius using atlas-based 2D/3D registration. Proc.SPIE **7261**, 7261 – 7261 – 9 (2009)
8. Issac, R.T., Gopalan, H., Abraham, M., John, C., Issac, S.M., Jacob, D.: Preoperative determination of tibial nail length: An anthropometric study. Chinese Journal of Traumatology **19**(3), 151 – 155 (2016)
9. Jiménez-Delgado, J.J., Paulano-Godino, F., PulidoRam-Ramírez, R., Jiménez-Pérez, J.R.: Computer assisted preoperative planning of bone fracture reduction: Simulation techniques and new trends. Medical Image Analysis **30**, 30 – 45 (2016)
10. Kelley, C.T.: Iterative methods for optimization. Frontiers in applied mathematics, SIAM, Philadelphia (1999)
11. Kistler, M., Bonaretti, S., Pfahrer, M., Niklaus, R., Büchler, P.: The Virtual Skeleton Database: An Open Access Repository for Biomedical Research and Collaboration. Journal of Medical Internet Research (2013)
12. Klima, O., Kleparnik, P., Spanel, M., Zemcik, P.: Intensity-based femoral atlas 2D/3D registration using Levenberg-Marquardt optimisation. Proc.SPIE **9788**, 9788 – 9788 – 12 (2016)
13. Klima, O., Novobilsky, P., Madeja, R., Barina, D., Chromy, A., Spanel, M., Zemcik, P.: Intensity-Based Nonoverlapping Area Registration Supporting "Drop-Outs" in Terms of Model-Based Radiostereometric Analysis. Journal of Healthcare Engineering **2018**, 1–10 (2018)
14. Klima, O., Chromy, A., Zemcik, P., Spanel, M., Kleparnik, P.: A Study on Performace of Levenberg-Marquardt and CMA-ES Optimization Methods for Atlas-based 2D/3D Reconstruction. IFAC-PapersOnLine **49**(25), 121 – 126 (2016), 14th IFAC Conference on Programmable Devices and Embedded Systems PDES 2016
15. Markelj, P., Tomaževič, D., Likar, B., Pernuš, F.: A review of 3D/2D registration methods for image-guided interventions. Medical Image Analysis **16**(3), 642 – 661 (2012), computer Assisted Interventions
16. Schumann, S., Bieck, R., Bader, R., Heverhagen, J., Nolte, L.P., Zheng, G.: Radiographic reconstruction of lower-extremity bone fragments: a first trial. International Journal of Computer Assisted Radiology and Surgery **11**(12), 2241–2251 (Dec 2016)
17. Smoger, L.M., Shelburne, K.B., Cyr, A.J., Rullkoetter, P.J., Laz, P.J.: Statistical shape modeling predicts patellar bone geometry to enable stereo-radiographic kinematic tracking. Journal of Biomechanics **58**, 187 – 194 (2017)
18. Valenti, M., De Momi, E., Yu, W., Ferrigno, G., Akbari Shandiz, M., Anglin, C., Zheng, G.: Fluoroscopy-based tracking of femoral kinematics with statistical shape models